SIN-CHN SCIENTIFIC PRESS PTE.LTD.

Molecular & Cellular Biomechanics 2025, 22(5), 646.
https://doi.org/10.62617/mcb646

Article

PD location and interference suppression method of power cable based on cross-correlation

Ningming Guo[1,2,*], Zhichang Feng[2], Dong Chen[2]

[1] College of electrical and Electronic Engineering, North China Electric Power University, Beijing 102206, China
[2] C-EPRI electrical Engineering co., ltd, NARI group, Beijing 102200, China
*** Corresponding author:** Ningming Guo, 70380822@qq.com.cn

CITATION

Guo N, Feng Z, Chen D. PD location and interference suppression method of power cable based on cross-correlation. Molecular & Cellular Biomechanics. 2025; 22(5): 646. https://doi.org/10.62617/mcb646

ARTICLE INFO

Received: 28 October 2024
Accepted: 12 November 2024
Available online: 24 March 2025

Abstract: A novel PD identification and location method based on cross-correlation is proposed in paper. The method aims to solve the problem of weak signal identification and interference suppression. Taking advantage of the characteristics that the time axis of PD pulses at both ends of the cable is symmetrical and the interference signal is asymmetric, the cross-correlation computation is carried out through the alignment of reference pulses, so as to suppress the interference effects such as corona. In the calculation of basis PD pulse time difference, the synchronous pulse actively injected is used to shorten the data time window and reduce the influence of noise, and the accurate time difference is extracted through generalized cross-correlation. In this paper, the above methods are verified by simulation and experiment. The analysis results show that the interference can be suppressed and the weak signal recognition ability can be improved through multiple correlation operations, which lays the foundation for accurate PD location.

Keywords: PD location; pulse interference; cross-correlation

1. Introduction

The partial discharge (PD) is an important factor affecting the safety of power cables. It is generally considered that the partial defects of insulation usually occur at cable accessories, but the operating experiences show that the partial defects of insulation may occur in the cable body due to foundation settlement, external puncture and other reasons.

Sometime the PD point is far away from the detection device, thus the location of PD source is necessary for insulation detection. When the power cable is long, the PD location mainly depends on the high-frequency component (below 30MHz) [1]. Because its frequency is close to corona and other interference, the method based on high-frequency component is relatively easy to be affected on site. The on-site interference can be divided into three types: periodic interference, pulse interference and white-noise interference [2]. Among them, the pulse interference is the harder one to solve. According to position of interference source, the pulse interference can be divided into:

1) External interference: the interference from outside of cable, such as corona, surface discharge.

2) Internal interference: the interference from inside of cable which is generally coupled to the cable by the adjacent conductors.

Due to longer length, the PD signal is always weaker at the end of cable. Furthermore, the interference is also superimposed with the PD signal at the same time. These factors increase the difficulty of PD identification and location. For long-distance cable, the identification of weak signal and interference suppression are need to solve at same time.

There are two types of algorithms for identification of weak signal. The most common algorithm is using the time-frequency analysis tools to extract weak signals by the decomposition of frequency band, such as wavelet transform [3,4], Hilbert Huang transform [5], stochastic resonance [6]. However, the time-frequency analysis can not distinguish PD signal from pulse interference because their waveform characteristics are similar. To solve the problem, some researchers proposed the algorithms based on statistics and cumulation analysis [7,8], the principle of such algorithms is the cumulant of noise is zero and the cumulant of PD signal is non-zero. However, such algorithms are not useful for early PD location because that the number of PD pulse is relatively weak at early stage. However, use clustering algorithm to improve the location accuracy by multiple PD pulse is still useful in engineering. This means that the location of PD source should not only improve the reliability of single PD pulse location and identification, but also improve the reliability of multiple weaker PD identification.

A novel PD location and identification method is proposed in paper. Its use cross-correlation computation to suppress the affection of pulse interference and enhance the weak PD signal at the same time. The method is verified by simulation and experiment.

2. PD recognition and location principle

2.1. Principle of PD location

The two-ended method based on the time difference has been widely used in PD location. Its principle is shown in **Figure 1**. When the PD detection devices are installed at both ends of cable, two end is named as M and N respectively. Where, t_m and t_n are the time that the PD pulse arrive the M and N, L is the total length of cable. The calculation formula is as follows:

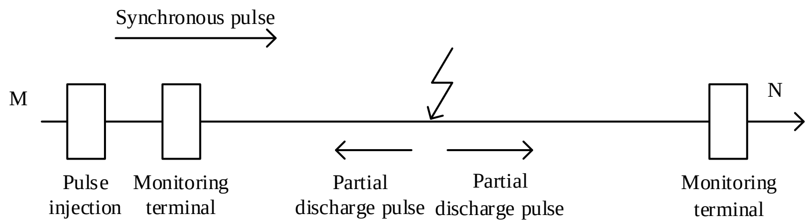

Figure 1. Principle of PD location principle.

$$l_1 = \frac{L-(t_m-t_n)v}{2}$$
$$l_2 = \frac{L-(t_n-t_m)v}{2} \quad (1)$$

In Equation (1), l_1 and l_2 are the distance from the PD point to two ends of the cable; and v is the wave velocity, the key point of calculation is the arriving time and wave velocity. Some references have proposed the setting algorithms of wave velocity [9,10]. The identification of weak signal, suppression of interference is mainly subject discussed in paper.

2.2. Interference suppression and identification

(1) Princple of cross-correlation

The cross-correlation means the similarity of the two signals, the calculation process is shown in **Figure 2**. For the signal $x(t)$ and the reference signal $y(t)$, the cross-correlation coefficient of them can be calculated by the following equation:

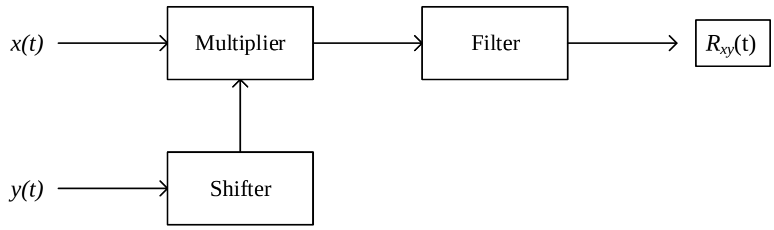

Figure 2. Principle of the cross-correlation computation.

$$x(t) = S_1(t) + n_1(t)\ y(t) = S_1(t) + n_2(t) \quad (2)$$

$$R_{xy}(t) = x(t)y(t+n) \quad (3)$$

In above formula, $S_1(t)$ is the signal to be extracted, $n_1(t)$ and $n_2(t)$ are the noise signals mixed with $S_1(t)$, $R_{xy}(t)$ is the cross-correlation coefficient of $x(t)$ and $y(t)$. It can be seen from formula 3 that the common parts of the $x(t)$ and $y(t)$ are enhanced through the multiplier, the irrelevant parts of $x(t)$ and $y(t)$ are suppressed. When the cross-correlation algorithm is used in PD location, $x(t)$ and $y(t)$ are the signals detected at both ends of cable. Another parameter of the cross-correlation computation is time-shift n, where n is the time difference of PD arriving time.

(2) External interference suppression

Assumed that the PD source generates PD pulse 1 at t_0, the time of PD pulse 1 transmit to M and N is t_m and t_n. Under these conditions, the instant that PD pulse 1 arrive M is: $t_0 + t_m$, the instant that PD pulse 1 arrive N is: $t_0 + t_n$. Assumed the external interference signal enters the cable at t_1, the instant that the external interference arrive N is $t_1 + t_m + t_n$. If PD pulse 1 is selected as the basis pulse, and use it to align the waveform of both ends, the aligned waveforms are shown in the **Figure 3a,b**.

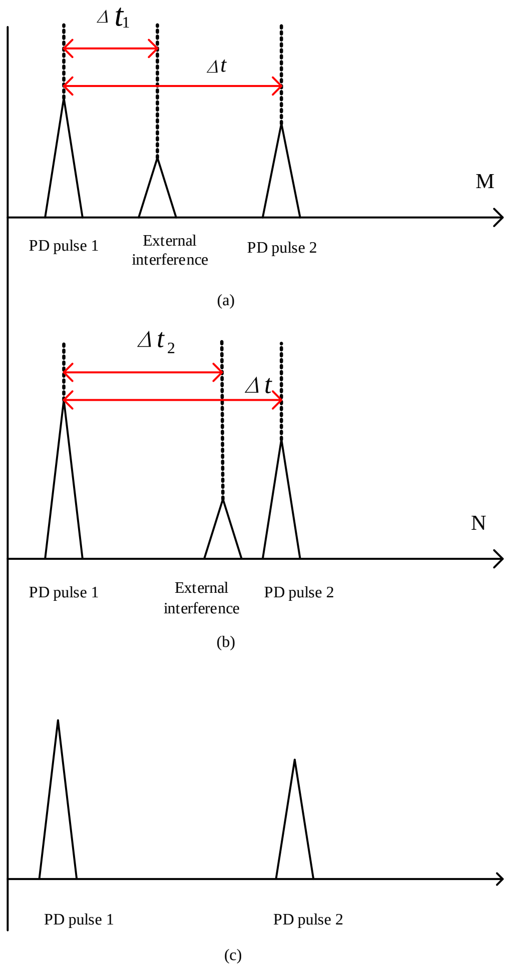

Figure 3. Principle of anti-interference based on cross- correlation.

At M end, the time difference between the PD pulse 1 and the interference signal is:

$$\Delta t_1 = t_1 - t_0 - t_m \quad (4)$$

At the N end, the time difference between PD pulse 1 and interference signal is:

$$\Delta t_2 = t_1 + t_m + t_n - t_0 - t_n \quad (5)$$

According to formular 4/5, there is a fixed deviation ($2 \times t_m$) between Δt_1 and Δt_2, it leads to the cross-correlation coefficient of interference will be reduced to zero in theory. Because PD pulse 2 is highly correlated at both ends, its amplitude will be enhanced through the cross-correlation computation. The cross-correlation coefficient of signals at both ends is show as **Figure 3c**.

(3) Internal interference suppression

Assumed that there is one interference signal coupled to cable at t_2, the time of interference signal transmit to both ends of the cable is t'_m and t'_n. The instant that the interference arrive M end is: $t_2 + t'_m$; the instant that the interference arrive N end is $t_2 + t'_n$. Other assumptions are same as those in the previous section. If the basis PD pulse (PD pulse 1) is aligned, the time difference between the PD pulse 1 and the interference signal at M end is

$$\Delta t'_1 = t_2 + t'_m - t_0 - t_m \quad (6)$$

At N end, the time difference between PD pulse 1 and interference signal is:

$$\Delta t'_2 = t_2 + t'_n - t_0 - t_n \quad (7)$$

As long as $t'_m - t_m \neq t'_n - t_n$, the cross-correlation coefficient of the internal interference will be zero, which is same to external interference. It means that the internal interference also can be suppressed by cross-correlation computation.

2.3. Calculation of time difference

From the perspective of signal processing, the calculation of arriving time is to find the singular point of the waveform. Wavelet transform and other time-frequency analysis approaches can figure out singular point by frequency-band decomposition, but it may be affected by the pseudo wave-peak. Due to the generalized cross-correlation uses the whole-waveform to detect the time difference of two signals, so it is less affected by the pseudo wave-peak. Furthermore, the generalized cross-correlation combined with filter can further improve signal-to-noise ratio. The calculation formula of the time-difference based on the generalized cross-correlation [11] is showed as:

$$n = argmax\, R_{x,y}\,(T) \quad (8)$$

where, n is the time difference of signal x and signal y, T is the analysis time-window. The whole signal length of PD signal is about tens of ns, but the length of recorded data in PD detection is often tens of millisecond. There may be multiple PD pulse signals. Use the whole recorded data to compute may lead to abnormal results, on the other side, it will take a long time, so it is necessary to shorten the time-window T.

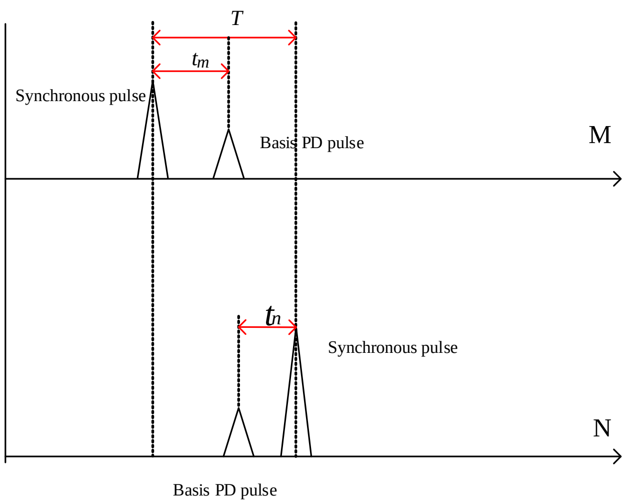

Figure 4. Identification of basis PD pulse.

Reference [15] proposed the active synchronization method in PD location, and it has been applied in many projects. Since the injected instant of synchronization pulse is controllable and its amplitude is relatively high. If the injected instant of synchronous pulse is controlled at the time that the phase of working votable is near 90° or 270°, while PD pulse signal is often generated. Assumed that the PD source generates basis PD pulse at t_0, and the synchronization pulse generator also generates a pulse signal at same time. At M end, the synchronization pulse is ahead of the basis PD pulse, and the time difference between the synchronization pulse and the basis PD pulse is: $\Delta t_m = t_m$. At N end, the synchronization pulse is behind of the basis PD pulse, and the time difference between them is $\Delta t_n = -t_n$. Therefore, the analysis time-window can be setted as $T = L/v$. The identification difficulty of PD pulse will be relatively lower in the time-windows. And the shorter time-windows also effectively reduce the of generalized cross-correlation computation and improve the calculation accuracy of time difference.

2.4. Algorithm flow

The flow of algorithm is as follows:

1) Pick out the basis PD pulse based on the synchronization pulse;

2) Use the basis PD pulse to align the waveform of both ends;

3) Cross-correlation computation combined with frequency domain filtering;

4) Use the cross-correlation coefficient and multiple PD pulse to figure out multiple initial results;

5) Using multiple results to locate PD point by clustering algorithm [15].

3. PSCAD simulation analysis

3.1. Simulation model

The performance of this PD location method was evaluated by simulation in PSCAD and the computational work was carried out via Matlab. The simulation model is shown in **Figure 5a** above and sampling frequency is 100MHz. The detailed geometry is illustrated in **Figure 5b** and the relevant cable parameters are refer to YJV22 8.7/15kV XLPE 185 cable.

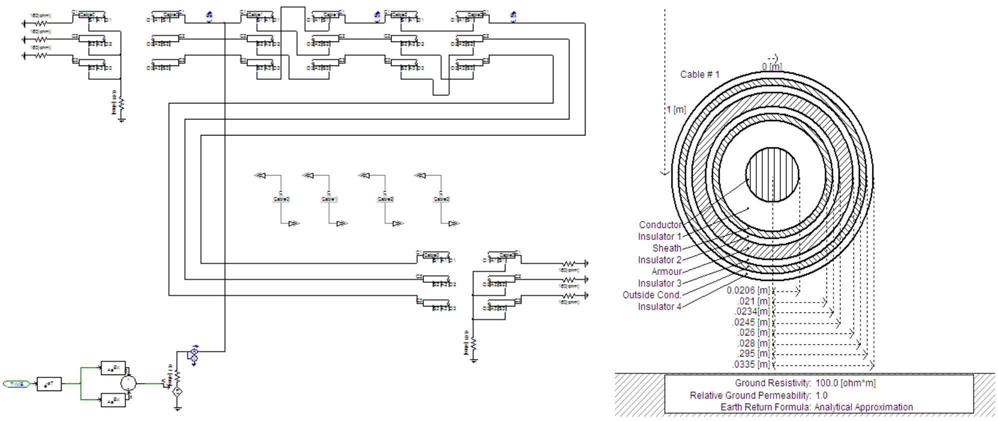

(a) System model **(b)** Cable model

Figure 5. Simulation model.

$$I(t) = I_0(e^{-\frac{t}{\tau_1}} - e^{-\frac{t}{\tau_2}}) \tag{9}$$

In simulation, the double exponential signal is adopted as the surge source, the wave front τ_1 and the wave tail τ_2 are set as 2 ns and 10 ns. The instantaneous amplitude of PD pulse 10 is 504 mA, thus the equivalent charge is about Q = 50 pC. The PD point is set in the middle of the cable, the PD point is 100 meters away from the M end and is 500 meters away from N end.

3.2. Results and analysis

(1) Enhancement of weak signal

Due to the attenuation of cable transmission, there is about 30% loss in the signal amplitude at the M/N. In order to, about 3dB white-noise is imposed on original signal. The signal waveform of M/N end under condition that adding white-noise is shown in **Figure 6a**. The original waveform is showed in **Figure 4a**. The signal after sliding windows is showed in **Figure 6b**.

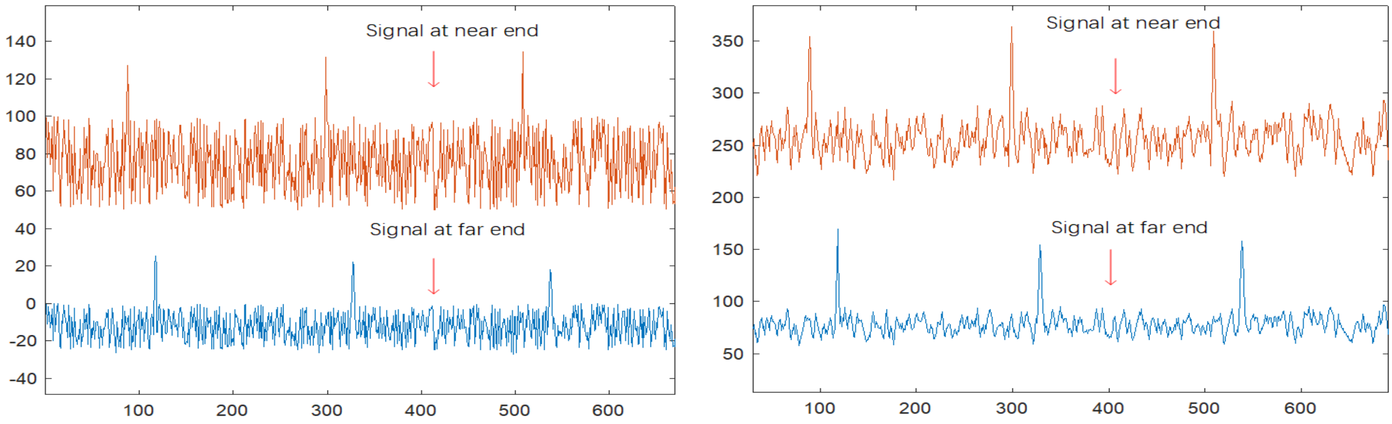

(a) Orignal signal. **(b)** Sliding windowing signal.

Figure 6. Signal comparison at both ends.

Note: The unit of X-axis is the sampling point, and unit of Y-axis is the code value.

Use B-spline wavelet transform to decompose the signal to obtain the detail coefficient in simulation. The detail coefficient is showed in **Figure 7a**, the waveform after cross-correlation computation is shown in **Figure 7b**. Each PD pulse is enhanced after frequency-domain filtering and cross-correlation computation. If adopt formula 10 to calculate, the signal-to-noise ratio is increased from 28dB to 47dB. The accuracy of PD location can be further improved through multiple clustering or averaging, it can reach the level within 5 m.

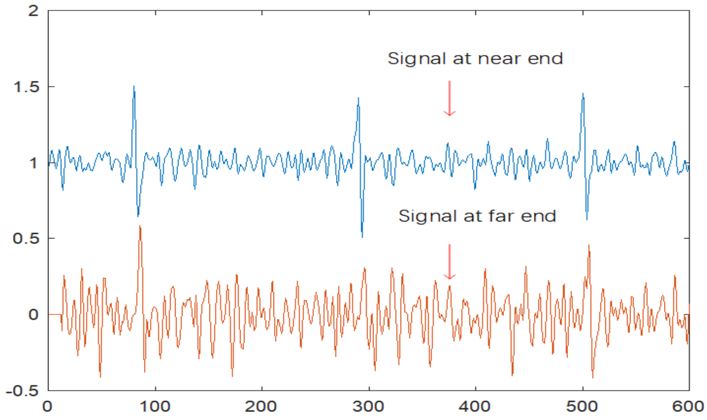

(a) Waveform of frequency domain filtered.

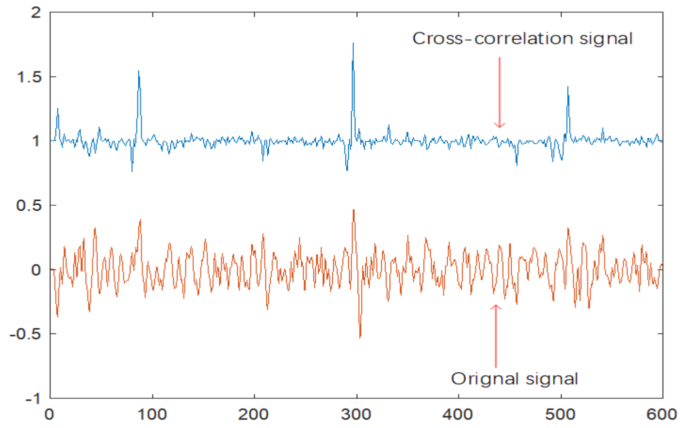

(b) Waveform of cross-correlation.

Figure 7. intermediate process of cross correlation processing.

$$\mathrm{SNR}=\frac{E(r(t)+s(t))}{E(s(t))} \tag{10}$$

(2) Suppression of pulse interference

To verify the effect of interference suppression, a pulse interference is imposed on original signal in simulation. As shown in the **Figure 8a,b**, the additional superimposed interference signal is not irrelevant in waveform. So, the pulse interference is suppressed after filter and cross- correlation process.

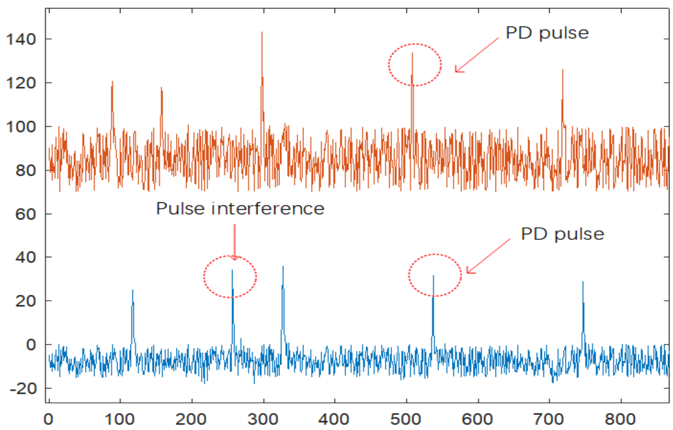

(a)

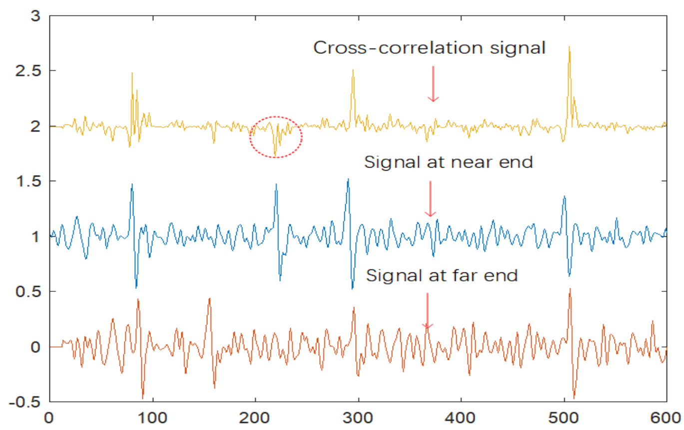

(b)

Figure 8. Intermediate process of cross correlation processing.

4. Experimental test

4.1. Experimental set-up

Figure 9 shows the Experiment test set-up. A YJV22 8.7/15kV XLPE 185 cable was used in the experiment and the length of cable is 250 m, the cable is unfolded in the experiment. The PD signal is manufactured by needling in the cable. The partial defects of insulation (PD point) is 25 m away from M end and it is 225 m away from N end. The synchronous pulse is injected as the reference timing signal through coupling coils. A pulse interference is produced by electronic igniter and it is coupled to cable. The sampling-frequency of detection device is 50MHz.

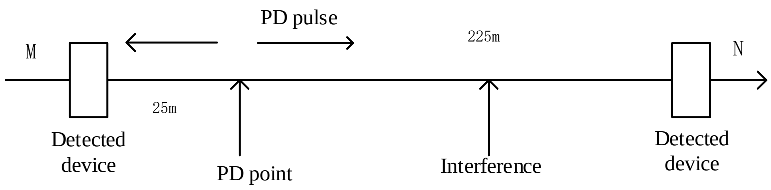

Figure 9. Setup of testing.

4.2. Result and analysis

In experiment, the waveform of PD signals detected at both ends of the cable is shown in **Figure 10a,b**. After a long-distance cable transmission, the amplitude of PD signal is significantly reduced and the peak of wave is smooth. The identification process of the basis PD pulse is showed as **Figure 11a,b**. At far end, basis PD pulse is advance synchronization pulse. At near end, the basic pulse is behind the synchronous pulse. The time-delay between the basis PD pulse and the subsequent pulse (PD pulse 2) is the same.

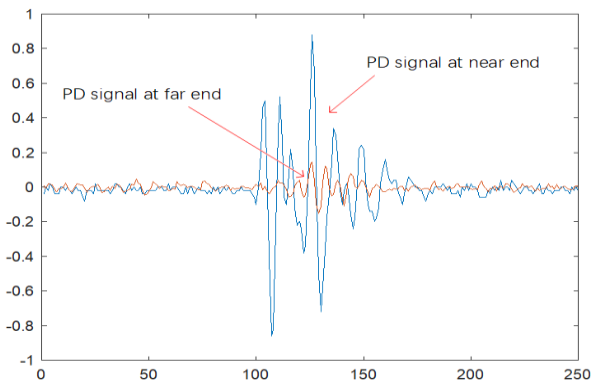

(a) Details waveform of PD signal.

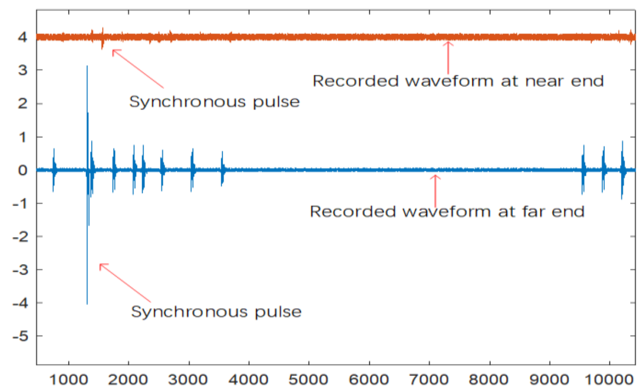

(b) Overall waveform of PD signal.

Figure 10. Comparison of original signals at both ends.

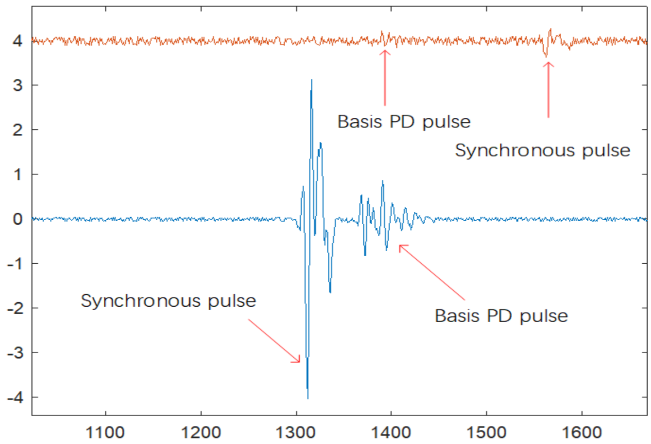

(a) Waveform at both ends.

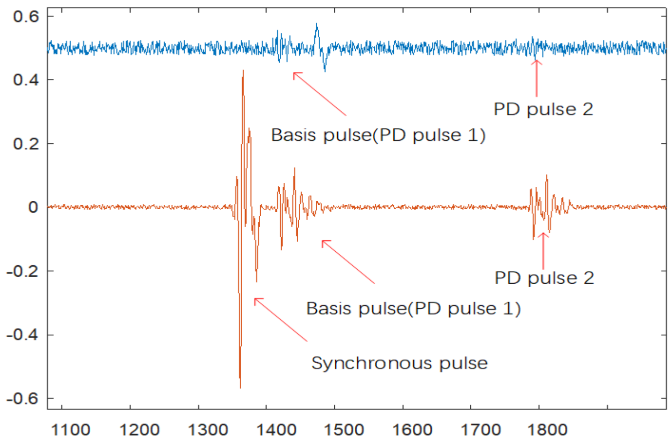

(b) Aligned waveform at both ends.

Figure 11. Comparison of far and near signals.

According to the conclusion in Section 2.3, the basic PD pulse is behind the synchronous pulse at near end, the basis PD pulse is advance to the synchronization pulse at far end. If the basis PD pulse can be picked out at near end. Assumed the time-difference of the basis PD pulse and synchronization pulse is Δt. At far end, the relative position of basis PD pulse should be fixed, which is advance to synchronization pulse about L/v-Δt. When the signals at both ends are aligned, the cross-correlation operation can be carried out, the comparison of cross- correlation coefficient and original signal are shown in **Figure 12a**. The weak signal is enhanced and the pulse interference is also suppressed at same time in **Figure 12b**. The location of PD can be further completed by using cross-correlation coefficient and clustering algorithm. In experiment, the accuracy of PD location can be less than 3 m, which is nearly to simulation result.

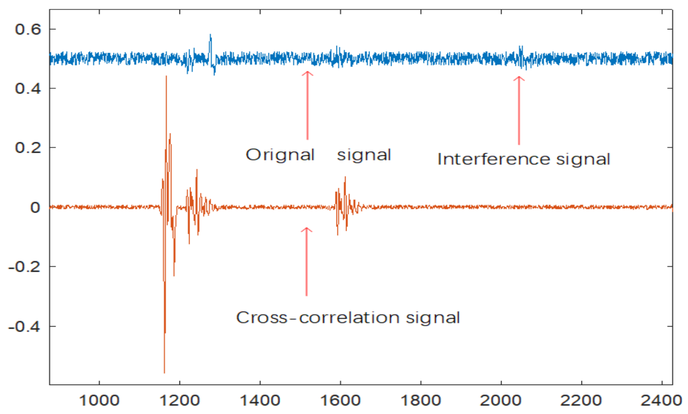

(a) Frequency domain cross-correlation data.

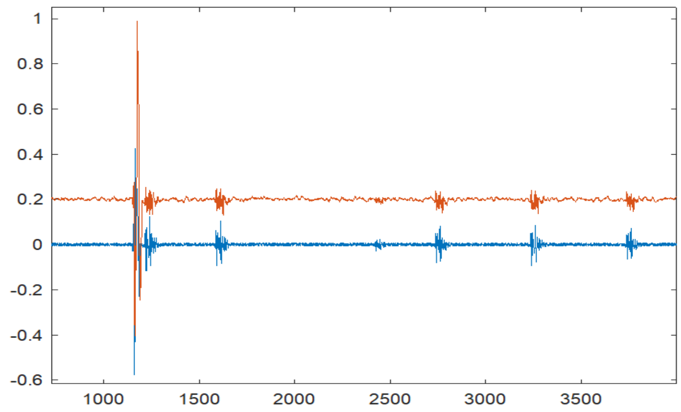

(b) original signal comparison.

Figure 12. Cross-correlation computation.

5. Influencing factors

5.1. Signal transmission dispersion

For the purpose of improving location accuracy, PD location is mainly based on high-frequency components, but different frequency signal transmission attenuation can lead to waveform distortion of the signal. Reference [16] proposed that the transmission process can be equivalent to a filtering process, in which the signals at both ends of the cable are converted into Equation (11):

$$\begin{aligned} r_1(t) &= s(t) + n_1(t) \\ r_2(t) &= H \bullet s(t-D) + n_2(t) \end{aligned} \tag{11}$$

In Equation (11), H represents the cable transmission equivalent filter. Obviously, this filtering process will reduce the correlation of signals $r_1(t)$ and $r_2(t)$. Reference [16] shows that and the degree of waveform distortion will further increase with the increase of line distance. So the method may be more suitable for shorter cables.

5.2. Filter design

The traditional wavelet transform generally uses convolution operation, and its filter coefficients are floating-point numbers. Thus, traditional wavelet transform has large amount of calculation and high complexity. If the proposed method is used for long-period data, it needs to consider the real-time operation. In order to improve the real-time performance of filtering, the lifting frame wavelet is proposed. The existing wavelet filter is decomposed into basic construction modules, and the wavelet transform is completed step by step, which is divided into the following three stages: decomposition, prediction and update, as shown in **Figure 13**.

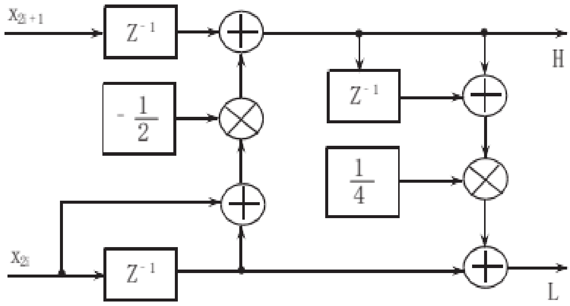

Figure 13. Process of lifting wavelet transform.

Taking 5/3 lifting wavelet as an example, its formula is as follows:

$$c(2n+1) = x(2n+1) - \left\lfloor \frac{x(2n) + x(2n+2)}{2} \right\rfloor \quad (12)$$

$$d(2n) = x(2n) - \left\lfloor \frac{c(2n-1) + c(2n+1) + 2}{4} \right\rfloor \quad (13)$$

In the above formula, $c(2n + 1)$ is detail coefficients of wavelet transform and $d(2n)$ are approximate coefficients. From Equations (12) and (13), it can be seen that the calculation of details and approximate coefficients is only “add and subtract” operation, and the division operation, which is completed by shift. In the FPGA hardware implementation, the same address operation is adopted without calling the system FIR filter core, which greatly improves the operation efficiency. In the test, when FPGA is used to process 20 ms recording time data with 50MHz sampling rate, the processing time of wavelet transform is less than 1ms. However, compared with the traditional wavelet transform, the lifting wavelet transform is solidified in hardware, its flexibility is limited to a certain extent, so it is necessary to optimize the design of filter passband in advance.

6. Conclusions

In PD location of the long-distance cable, two problems are need to be solved at same time. On one hand, the pulse interferences such as corona are need to suppressed. On the other hand, the weak PD signal mixed with white-noise is also needed to enhanced. To solve the two problems, a novel method for cable PD location based on cross- correlation is proposed in paper. Its principle is as follows:

1) The PD signals at both ends are correlated, while the interference signals are not correlated with each other.

2) Using the synchronization pulse injected actively can identify the basis PD pulse and shorten the time-window of generalized cross-correlation computation, so as to reduce the influence of pulse interference.

3) The signal-to-noise ratio can be improved by frequency-domain filtering and cross-correlation computation.

The above methods are verified by simulation and experiment in paper, which lays a foundation for improving the accuracy and reliability of PD location.

Conflict of interest: The authors declare no conflict of interest.

References

1. Zhang Wei, Zhang Long, Huang Zhiwei, et al. Time domain analysis of partial discharge propagation in cross-linked polyethylene cables considering frequency-dependent parameters. High Voltage Engineering, 2014, 40(11): 3461-3467.
2. LI Junhao, HAN Xutao, LIU Zehui, et al.Review on partial discharge measurement technology of electrical equipment. High Voltage Engineering, 2015, 41(8): 2583-2601.
3. Du Yan，Liao Ruijin，Zhou Quan，etal．Study on time delay estimation algorithm in cable partial discharge location based on wavelet transform．High Voltage Apparatus,2007,10(5): 389-393．
4. Zhang Ruobing, Jin Sen, Du Gang. Method of partial discharge localization for cable under oscillatory wave voltage conditions based on EMD and DTW algorithm. High Voltage Engineering, 2020, 46(1): 273-281.
5. Herold C，Leibfried T，Markalous S，etal．Algorithms for automated arrival time estimation of partial discharge signals in power cables, International Symposium on High Voltage Engineering ，Ljubljana,2007：327-332．
6. Mardiana R,Su C Q．Partial discharge location in power cables using a phase difference method．IEEE Transactions on Dielectrics and Electrical Insulation，2010，17(6)：1738-1746．
7. Liu Weidong，Liu Shanghe，Hu Xiaofeng，et al．Aperiodic weak partial discharge source detection based on accumulation of cross correlation estimation information．High Voltage Engineering，2017，43(3)：966-972．
8. HOU Huijuan, SHENG Gehao, ZHU Wenjun, et al. Time-delay estimation algorithm of partial discharge ultra high frequency signals based on higher-order cumulant. High Voltage Engineering, 2013, 39(2): 342-347.
9. FU Ling, LIU Hong, LIN Shen, etal Multi-source PD Location Algorithm Considering PD Signal Propagation Characteristics．High Voltage Engineering，2017,43(12)：4060-4069.
10. Gao Shuguo，Liu Hechen，Fan Hui，etal．PD location method of power cable based on wavelet transform modulus maxima considering wave characteristics．Power System Technology，2016，40(7)：2244-2250．
11. Hu Xiaofeng，Liu Weidong，Wanglei，etal．Time-delay estimation of corona discharge radiation signal based on generalized cross correlation. High Power Laser and Particle Beams，2018，30(1)：56-60.
12. Xie Min，Zhou Kai，Zhao Shilin，etal．A new location method of local defects in power cables based on reflection coefficient spectrum ．Power System Technology，2017，9(9)：3083-3089．
13. WANG Ganjun, LI Jinshu, WU Yijiang, etal. Random Forest Based Feature Selection for Partial Discharge Recognition of HV Cables．Power System Technology，2019，43(4)：1329-1335．
14. Tang Ju，Chen Jiao，Zhang Xiaoxing，et al．Time difference algorithm based on energy relevant search of multi-sample applied in PD location．Proceedings of the CSEE，2009，29(19)：125-130．
15. HU Yue,SI Liangqi, ZHANG Weidong, etal. Phase synchronization based on independent reference pulse for online UHF PD detection.Electric power automation equipment, 2013, 33(11) 44-49.
16. LEI Liu, LI Zewen, XIA Yixiang, et al.A precise detection method for traveling waves based on adaptive black box inversion. Automation of Electric Power Systems, 2022, 46 (15): 128-135.